J. Phys. B: At. Mol. Opt. Phys. **29** (1996) 2497–2514. Printed in the UK

Electron capture, excitation and ionization in slow collisions of Li^{3+} ions with ground-state and metastable hydrogen atoms

R K Janev†, E A Solov'ev‡‖ and Yi Wang§

† International Atomic Energy Agency, PO Box 100, A-1400 Vienna, Austria
‡ Macedonian Academy of Sciences and Arts, PO Box 428, 91000 Skopje, Macedonia
§ Institute of Applied Physics and Computational Mathematics, PO Box 8009, Beijing 100088, People's Republic of China

Received 20 October 1995, in final form 5 March 1996

Abstract. Using the advanced adiabatic method we have calculated the cross sections for excitation, ionization and electron capture of H(1s) and H(2s) colliding with Li^{3+} in the energy ranges 0.1–20 keV/u and 0.1–7 keV/u, respectively. All radial and rotational couplings among the adiabatic states with united atom principal quantum number $N \leqslant 10$ have been included in the calculations, as well as the electron promotion to the continuum via the S- and Q-superseries of hidden crossings. The obtained results are compared, when possible, with the results of other cross section calculations or measurements.

1. Introduction

There is a growing interest in current fusion research in the use of lithium beams and lithium pellets for diagnostics of tokamak edge plasma parameters (Aumayr *et al* 1992) and fusion-born alpha particle velocity distribution (Fisher *et al* 1995), respectively. The transport of ionized lithium atoms in the plasma, particularly at its cold periphery, is significantly affected by their collisions with the neutral hydrogen gas. In the present article we shall consider the inelastic collision processes (electron capture, excitation and ionization) of Li^{3+} ions with ground-state and metastable hydrogen atoms, H(1s) and H(2s), at low collision energies (below 20 keV/u for H(1s) and below 7 keV/u for H(2s)).

Previous theoretical studies of $Li^{3+} + H(1s)$ collision system in the low-energy region concentrated mainly on the electron transfer process and were motivated by the electron capture cross section measurements of Seim *et al* (1981) performed in the 0.57–6 keV/u energy range. The most extensive molecular orbital (MO)-based close-coupling calculations for electron capture in this collision system were performed by Kimura and Thorson (1983) with a 10 MO basis set, and by Salin (1982) with a 24 MO basis (which includes all the states with united atom principal quantum number $N \leqslant 4$). The most elaborate atomic orbital (AO)-based close-coupling calculations were performed by Bransden and Noble (1982) with a 20 AO basis, and by Fritsch and Lin (1982) with a 24 AO+ basis (the 1s orbital on H, all $n = 2$ and $n = 3$ orbitals on Li^{2+} and the 2s, 2p, 3s and 3d united atom (Be^{3+}) orbitals on both nuclei). We should mention also the close-coupling calculations of Lüdde and Dreizler (1982) employing 100–150 two-centre pseudostates. All these calculations have achieved a good overall description of the process, with a satisfactory agreement of the total electron

‖ On leave of absence from the Department of Theoretical Physics, Institute of Physics, University of St Petersburg, St Petersburg 198904, Russia.

0953-4075/96/122497+18$19.50

capture cross section with the experimental data (within the uncertainty of the latter). State-selective electron capture cross sections were reported only by Bransden and Noble (1982) and Fritsch and Lin (1982) for the $2l$ and $3l$ Li^{2+} states, and cross sections for excitation of hydrogen atom to its $2l$ and $3l$ states were given by Bransden and Noble (1982) only.

The inelastic processes in $Li^{3+} + H(2s)$ collisions at low energies have not been extensively studied so far. The only available theoretical study is that of Casaubon and Piacentini (1984) for the electron capture in this system, which was performed within the Landau–Zener model using exact adiabatic energies. Only two, mutually independent reaction channels were included in this study, each of the channels containing one pair of strongly coupled molecular states ($6h\sigma$–$5g\sigma$ and $5f\sigma$–$4d\sigma$).

The present study of $Li^{3+} + H(1s)$, H(2s) collisions at low energies is aimed at providing more detailed information on the collision dynamics of this system and quantitative cross section information for the most important excitation, ionization and electron capture reaction channels. We shall employ the advanced adiabatic approach to ion–atom collisions which describes the dynamical evolution of the system in terms of analytical properties of adiabatic electron energies in the complex plane of internuclear distance R, includes all the couplings between the states within a chosen molecular basis and incorporates the effects of electron translational motion (i.e. it is formulated on a dynamical adiabatic molecular basis compatible with the physical boundary conditions). A full description of the method is given elsewhere (Solov'ev 1989). One of the specific features of the method is that it allows a unified description of the reaction channels both within the discrete spectrum and in the continuum (including the energy distribution of emitted electrons). Elaborate applications of the advanced adiabatic method have so far been done for the collision systems $H^+ + H$ ($n \leqslant 4$) (Janev and Krstić 1992), $He^{2+} + H$ (n) (Grozdanov and Solov'ev 1990, $n \leqslant 2$; Solov'ev 1991, $n = 1$; Krstić and Janev 1993, $n \leqslant 4$) and Be^{4+}, $B^{5+} + H$ ($n \leqslant 2$) (Krstić *et al* 1992). The molecular basis in the calculations of Janev and Krstić (1992), Krstić and Janev (1993) and Krstić *et al* (1992) included all the states with united atom principal quantum number $N \leqslant 9$ and selected states with $N = 10$ and $N = 11$.

The treatment of the collision dynamics of the Li^{3+}–H system in the present work will be carried out at the same level of complexity: all the couplings (radial and rotational) among the molecular states with $N \leqslant 10$ will be included in the dynamics. This basis allows one to describe all the processes in the system leading to population of the separated atom states with $n \leqslant 2$ (and of some with $n = 3$) on the H atom and the states with $n \leqslant 9$ on the Li^{2+} ion, where n is the separated atom principal quantum number. The states with $N > 10$ are considered as lying in the continuum.

The organization of the paper is as follows. In section 2 we discuss the structure of the 'hidden crossings' of adiabatic potential energy surfaces of the system $Li^{3+} + H$ in the complex R-plane. In section 3 we provide a brief account of the method used for calculation of the cross sections of inelastic processes in this system. In section 4 we give the cross section results for excitation, ionization and electron capture in $Li^{3+} + H(1s)$ collisions, whereas in section 5 we present the cross section results for these processes in $Li^{3+} + H(2s)$ collisions. In section 6 we give some concluding remarks.

Atomic units ($e = m_e = \hbar = 1$) will be used throughout this work, unless otherwise explicitly stated.

2. Structure of adiabatic energy hidden crossings in the Li^{3+}–H system

The solution of the adiabatic eigenvalue problem for the one electron–two Coulomb centre system (Z_1, e, Z_2) in the complex plane of internuclear distance R (Z_1, Z_2 are the nuclear

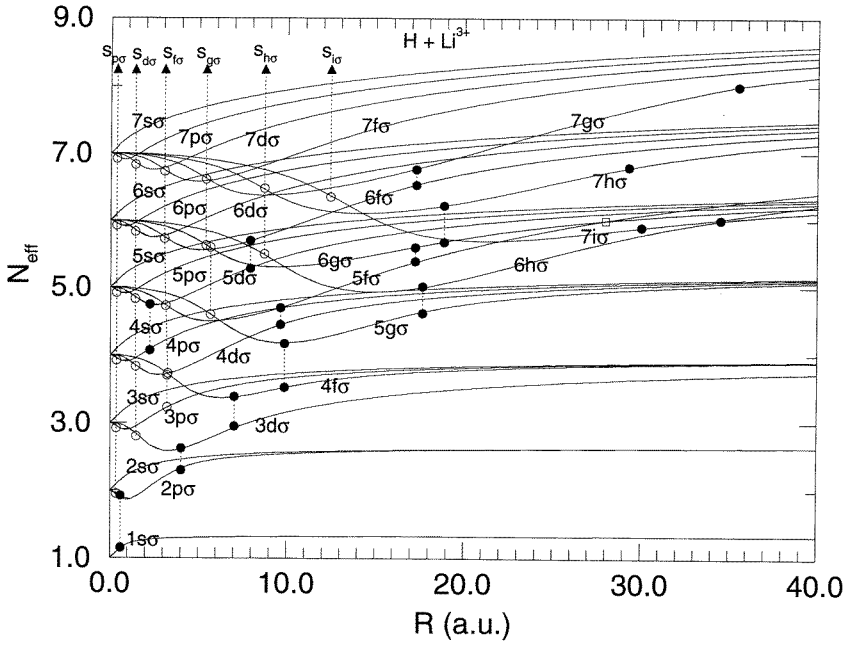

Figure 1. Dependence of effective principal quantum number $N_{\text{eff}} = 4/(-2E)^{1/2}$ on internuclear distance for the Li^{3+}–H system. The real parts of the positions of S- and Q-branch points are shown by open and full circles, respectively. The open square connecting the 5fσ and 6gσ 'potential curves' indicates the position of their 'true' avoided (Landau–Zener) crossing.

charges) reveals that the potential energy surfaces of adiabatic states having the same symmetry are mutually pairwise connected by a number of square-root branching points, thus forming a multiply connected Riemann surface $E(R)$ (Solov'ev 1981, Ovchinnikov and Solov'ev 1986, Janev and Krstić 1991). When close enough to the real R-axis, these branching points ('hidden crossings') appear as avoided crossings of the corresponding potential energy curves on the ReE–ReR plane. The investigations of the topology of adiabatic energy Riemann surface of (Z_1, e, Z_2) system further revealed that the branching points form series with certain characteristic features. In the asymmetric systems, $Z_1 \neq Z_2$, two basically different types of series of branching points have been identified: S- and Q-series.

The branch points of a S-series connect the molecular states $|Nlm\rangle$ and $|N+k, lm\rangle$, $k = 1, 2, 3, \ldots$ where N, l, m are the usual spherical quantum numbers in the united atom limit. From the point of view of electronic transitions, only the first branch points ($k = 1$) of the S-series are important. The first terms of the S-series form, on their own, series (or superseries) S_{lm} which connect the states $|Nlm\rangle$ and $|N+1, lm\rangle$ consecutively for all $N \geqslant l+1$. The branch points $R^{(S)}_{Nlm}$ of a superseries S_{lm} satisfy the relations $\text{Re}R^{(S)}_{N+1,lm} < \text{Re}R^{(S)}_{Nlm}$, $\text{Im}R^{(S)}_{N+1,lm} < \text{Im}R^{(S)}_{Nlm}$, all are located in a small region Ω_{lm} in the complex R-plane (not far from the coordinate origin), and have a limit point $R^{(S)}_{lm} = \lim_{N\to\infty} R^{(S)}_{Nlm}$ at the continuum edge. Because of these features, the collision system reaching a S_{lm} superseries in the incoming stage of the collision is rapidly promoted to the continuum ('superpromotion').

The branch points of a Q-series connect the molecular state $|Nlm\rangle$ with the higher states

Table 1. Positions and Massey parameters of branch points of the S_{lm} superseries in the $Li^{3+}+H$ system.

Superseries	$Re R_c$; $Im R_c$	Δ_0	Superseries	$Re R_c$; $Im R_c$	Δ_0
$S_{p\sigma}$			$S_{d\pi}$		
2pσ–3pσ	0.351; 0.585	0.6438	3dπ–4dπ	0.604; 1.700	0.6427
3pσ–4pσ	0.347; 0.562	0.2197	4dπ–5dπ	0.602; 1.608	0.2858
4pσ–5pσ	0.343; 0.551	0.1001	5dπ–6dπ	0.599; 1.571	0.1526
5pσ–6pσ	0.343; 0.550	0.0544	6dπ–7dπ	0.596; 1.552	0.0912
6pσ–7pσ	0.342; 0.548	0.0326	7dπ–8dπ	0.595; 1.541	0.0589
7pσ–8pσ	0.341; 0.547	0.0211	8dπ–9dπ	0.593; 1.534	0.0402
8pσ–9pσ	0.341; 0.546	0.0145	$S_{f\pi}$		
$S_{d\sigma}$			4pf–5fπ	2.294; 2.765	0.4962
3dσ–4dσ	1.492; 1.080	0.4451	5fπ–6fπ	2.215; 2.591	0.2558
4dσ–5dσ	1.441; 1.010	0.1933	6fπ–7fπ	2.175; 2.513	0.1502
5dσ–6dσ	1.419; 0.983	0.1018	7fπ–8fπ	2.152; 2.471	0.0959
6dσ–7dσ	1.406; 0.970	0.0602	8fπ–9fπ	2.136; 2.446	0.0651
7dσ–8dσ	1.399; 0.963	0.0386			
8dσ–9dσ	1.394; 0.958	0.0262	$S_{g\pi}$		
$S_{f\sigma}$			5gπ–6gπ	4.666; 3.820	0.3831
4fσ–5fσ	3.256; 1.596	0.3143	6gπ–7gπ	4.470; 3.567	0.2174
5fσ–6fσ	3.126; 1.475	0.1578	7gπ–8gπ	4.369; 3.447	0.1365
6fσ–7fσ	3.064; 1.424	0.0912	8gπ–9gπ	4.307; 3.379	0.0916
7fσ–8fσ	3.028; 1.396	0.0577			
8fσ–9fσ	3.005; 1.380	0.0388	$S_{h\pi}$		
$S_{g\sigma}$			6hπ–7hπ	7.707; 4.874	0.3023
5gσ–6gσ	5.660; 2.142	0.2321	7hπ–8hπ	7.363; 4.546	0.1837
6gσ–7gσ	5.419; 1.962	0.1284	8hπ–9hπ	7.179; 4.383	0.1213
7gσ–8gσ	5.296; 1.881	0.0795			
8gσ–9gσ	5.222; 1.835	0.0528	$S_{i\pi}$		
$S_{h\sigma}$			7iπ–8iπ	11.408; 5.934	0.2440
6hσ–7hσ	8.721; 2.716	0.1782	8iπ–9iπ	10.895; 5.533	0.1561
7hσ–8hσ	8.336; 2.472	0.1058			
8hσ–9hσ	8.130; 2.356	0.0689	$S_{j\pi}$		
$S_{i\sigma}$			8jπ–9jπ	15.771; 7.007	0.2009
7iσ–8iσ	12.444; 3.315	0.1411			
8iσ–9iσ	11.888; 3.002	0.8840	$S_{g\sigma}$		
$S_{j\sigma}$			5gσ–6gσ	3.006; 4.968	0.4763
8jσ–9jσ	16.837; 3.935	0.1145	6gσ–7gσ	2.911; 4.657	0.2729
			7gσ–8gσ	2.858; 4.507	0.1724
			8gσ–9gσ	2.825; 4.420	0.1162
			$S_{h\sigma}$		
			6hσ–7hσ	5.962; 6.607	0.3876
			7hσ–8hσ	5.716; 6.187	0.2384
			8hσ–9hσ	5.582; 5.976	0.1585
			$S_{i\sigma}$		
			7iσ–8iσ	9.614; 8.225	0.3194
			8iσ–9iσ	9.190; 7.705	0.2069

$|N+k, l+k, m\rangle$, $k = 1, 2, 3, \ldots$. With increasing k, the imaginary part of the branching points of a Q-series increases by (roughly) a constant amount, while their real part remains almost unchanged. Therefore, from the point of view of electronic transitions, only the first term, $k = 1$, of a Q-series is important. The first terms of Q-series form, on their own, new series, Q-superseries, which connect the states $|Nlm\rangle$ and $|N+1, l+1, m\rangle$ pairwise

and successively. The branching points $R^{(Q)}_{Nlm;N+1,l+1,m}$ of a Q-superseries are characterized by the relation $\mathrm{Re}R^{(Q)}_{Nlm;N+1,l+1,m} < \mathrm{Re}R^{(Q)}_{N+1,l+1,m;N+2,l+2,m}$ and, therefore, a Q-superseries provides a path for promotion of the system to states with higher N (and to the continuum) during the outgoing stage of the collision.

The probability for transition from one adiabatic state $|\alpha\rangle$ to another $|\beta\rangle$, connected by a branching point R_c, is given, at an adiabatically low collision velocity v, by (see e.g. Solov'ev 1989)

$$p_{\alpha\beta} = \exp\left(-\frac{2}{v}\Delta_{\beta\alpha}\right) \tag{1}$$

where $\Delta_{\beta\alpha}$ is the generalized Massey parameter defined by

$$\Delta_{\beta\alpha} = \left|\mathrm{Im}\int_{\mathrm{Re}x(R_c)}^{x(R_c)} \Delta E_{\beta\alpha}(R(x))\,\mathrm{d}x\right|. \tag{2}$$

$\Delta_{\beta\alpha}(R) = E_\beta(R) - E_\alpha(R)$ is the difference of the energies of adiabatic states $|\beta\rangle$ and $|\alpha\rangle$, $x = vt = (R^2 - b^2)^{1/2}$ (in a straightline approximation for the classical trajectory), and b is the impact parameter. The integral (2) is calculated along a contour in the complex R-plane, which connects the real axis and the branch point. In the straightline trajectory approximation and for $b \ll |R_c|$, $\Delta_{\beta\alpha}$ can be expanded as

$$\Delta_{\beta\alpha}(b) \simeq \Delta_{\beta\alpha}(0)\left(1 + \frac{b^2}{2|R_c|^2}\right) \tag{3}$$

where $\Delta_{\beta\alpha}(0) = \Delta_0$ is the value of the integral (2) for $b = 0$. The quantity Δ_0 is an important characteristic of the branching point R_c connecting the states $|\alpha\rangle$ and $|\beta\rangle$; according to equation (1) it represents a measure of adiabaticity of the transition.

Using the existing computer programs (Solov'ev 1991), we have solved the adiabatic eigenvalue problem for the system Li^{3+}–H in the complex R-plane with a basis containing all $N \leqslant 10$ states, we have determined the positions of branching points of all S- and Q-superseries appearing in this molecular basis and calculated the corresponding generalized Massey parameters, $\Delta_{\beta\alpha}(b)$. Figure 1 shows the dependence of effective principal quantum number $N_{\mathrm{eff}} = (Z_1 + Z_2)/(-2E)^{1/2} = 4(-2E)^{-1/2}$ on $\mathrm{Re}R$ for the σ-states with $N \leqslant 7$. The values $\mathrm{Re}R_c$ for the first several members of some S- and Q-superseries are also shown in this figure to indicate the transition region between particular states. More detailed information on the branch points of most important S- and Q-superseries, including the values of corresponding Massey parameters Δ_0, is given in table 1 and table 2. In table 2, we give also the parameters of a number of isolated branching points corresponding to the avoided (Landau–Zener) crossings; they are denoted by an asterix. The positions of the first several branch points of some of the S- and Q-superseries are also shown in figures 2 and 3, respectively. The branch points with $\mathrm{Re}R > 30$ and small values of Δ_0 in figure 3 represent the avoided Landau–Zener crossings, and they are visibly separated from the other points.

As can be seen from table 1, the values of Massey parameters $\Delta_0^{(S)}$ of a given S_{lm} superseries decrease rapidly with increasing N. For sufficiently high members of the superseries ($N \gg N_0$), $\Delta_0^{(S)}$ can be estimated by (using certain relations given in Solov'ev 1981, 1986)

$$\Delta_0^{(S)} \simeq \frac{(Z_1 + Z_2)}{N^3}(m+1)[2(l+1/2)^2 - \tfrac{1}{4}(m+1)^2]^{1/2}. \tag{4}$$

Table 2. Positions and Massey parameters of branch points of Q_{nlm} superseries in the $Li^{3+} + H$ system.

Superseries	ReR_c; ImR_c	Δ_0	Superseries	ReR_c; ImR_c	Δ_0
$Q_{1s\sigma}$			$Q_{2p\pi}$		
1sσ–2pσ	0.596; 0.980	2.7856	2pπ–3dπ	1.721; 2.582	1.3321
2pσ–3dσ	4.016; 1.561	0.3535	3dπ–4fπ	6.047; 3.725	0.4996
3dσ–4fσ	7.034; 4.009	0.6551	4fπ–5gπ	13.293; 3.797	0.1353
4fσ–5gσ	9.869; 4.465	0.6337	5gπ–6hπ	23.287; 9.113	0.0936
5gσ–6hσ	17.657; 4.457	0.1763	*5gπ–6hπ	30.999; 0.4679	0.0002
6hσ–7iσ	29.239; 9.936	0.0495	6hπ–7iπ	24.095; 8.824	0.2873
*6hσ–7iσ	34.507; 1.108	0.00145	7iπ–8jπ	34.963; 7.690	0.1022
7iσ–8jσ	30.019; 9.748	0.3237	*8jπ–9kπ	52.644; 4.406	0.0115
8jσ–9kσ	41.314; 8.443	0.1183	$Q_{3p\pi}$		
$Q_{2s\sigma}$			3pπ–4dπ	< 0;	—
2sσ–3pσ	< 0;	—	4dπ–5fπ	5.627; 5.269	0.3801
3pσ–4dσ	3.224; 2.806	0.3750	5fπ–6gπ	12.600; 6.223	0.1866
4dσ–5fσ	9.640; 3.104	0.1005	6gπ–7hπ	22.746; 5.811	0.0655
5fσ–6gσ	17.245; 8.317	0.1323	*7hπ–8iπ	40.559; 2.381	0.0030
6gσ–7hσ	18.867; 7.850	0.2508	8iπ–9jπ	36.972; 13.381	0.1552
7hσ–8iσ	29.198; 6.896	0.0871	$Q_{4p\pi}$		
*8iσ–9jσ	46.634; 3.550	0.00721	4pπ–5dπ	< 0;	—
$Q_{3s\sigma}$			5dπ–6fπ	4.580; 6.291	0.2746
3sσ–4pσ	< 0;	—	6fπ–7gπ	11.605; 8.197	0.1765
4pσ–5dσ	2.248; 2.994	0.2297	7gπ–8hπ	21.248; 8.867	0.0968
5dσ–6fσ	7.920; 4.799	0.1384	8hπ–9iπ	34.280; 7.958	0.0391
6fσ–7gσ	17.298; 4.754	0.0478	$Q_{5p\pi}$		
7gσ–8hσ	30.084; 13.288	0.0390	5pπ–6dπ	< 0;	—
*7gσ–8hσ	35.514; 1.349	0.00091	6dπ–7fπ	3.450; 6.321	0.1860
8hσ–9iσ	29.871; 11.641	0.1346	7fπ–8gπ	10.012; 9.482	0.1485
$Q_{4s\sigma}$			8gπ–9hπ	19.576; 11.309	0.1012
4sσ–5pσ	< 0;	—	$Q_{3d\delta}$		
5pσ–6dσ	1.922; 2.758	0.1275	3dδ–4fδ	3.353; 4.785	0.8669
6dσ–7fσ	6.281; 5.095	0.1098	4fδ–5gδ	8.856; 6.388	0.4504
7fσ–8gσ	14.584; 6.921	0.0708	5gδ–6hδ	16.724; 7.166	0.2162
8gσ–9hσ	26.954; 6.519	0.0282	6hδ–7iδ	27.731; 6.619	0.0783
$Q_{5s\sigma}$			*7iδ–8jδ	45.782; 3.205	0.0056
5sσ–6pσ	< 0;	—	$Q_{4d\delta}$		
6pσ–7dσ	1.816; 2.632	0.7631	4dδ–5fδ	< 0;	—
7dσ–8fσ	5.555; 4.762	0.0744	5fδ–6gδ	8.539; 8.268	0.3454
8fσ–9gσ	12.186; 7.354	0.06354	6gδ–7hδ	16.530; 9.724	0.2082
$Q_{6s\sigma}$			7hδ–8iδ	27.070; 10.133	0.1127
6sσ–7pσ	< 0;	—	8iδ–9jδ	40.943; 9.048	0.0471
7pσ–8dσ	1.767; 2.563	0.0491	$Q_{5d\pi}$		
8dσ–9fσ	5.246; 4.533	0.0511	5dπ–6fπ	< 0;	—
$Q_{7s\sigma}$			6fπ–7gπ	7.614; 9.815	0.2651
7sσ–8pσ	< 0;		7gπ–8hπ	15.787; 12.026	0.1845
8pσ–9dσ	1.734; 2.519	0.0334	8hπ–9iπ	26.306; 13.245	0.1195

The limit point $R_{lm}^{(S)}$ of a S_{lm} superseries can be obtained by using the modified semiclassical approximation and is given by (Solov'ev 1986)

$$R_{lm}^{(S)} \simeq \frac{1}{(Z_1+Z_2)}\{(l+1/2)^2 - \tfrac{1}{2}(m+1)^2 \pm \mathrm{i}(m+1)[2(l+1/2)^2 - \tfrac{1}{4}(m+1)^2]^{1/2}\}. \quad (5)$$

These endpoints of the S_{lm} superseries are not shown in figure 2. It should be remarked that

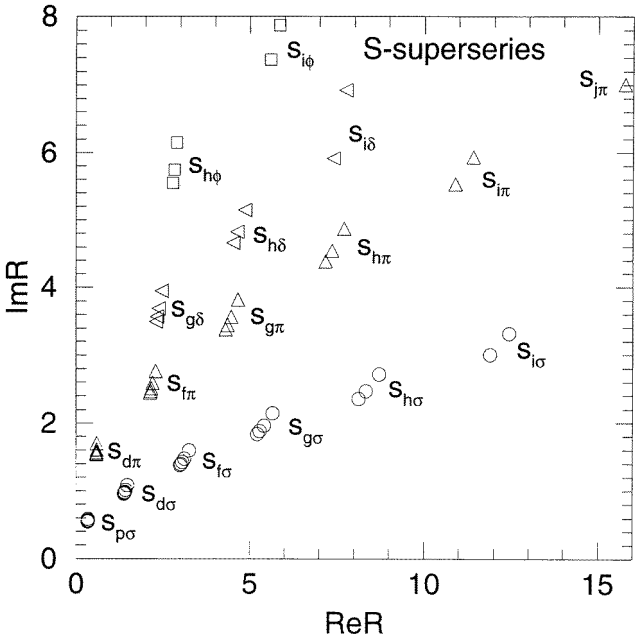

Figure 2. Positions of branching points $R_c^{(S)}$ of several S_{lm} superseries in the complex R-plane. The point with largest $\mathrm{Re}R_c^{(S)}$ within a given superseries represents the first term of that superseries.

the steepness of the S_{lm} superseries decreases with increasing l (for a fixed value of m) and increases with increasing m (for a given value of l). This parameter defines the strength of the promotive character of a S_{lm} superseries. Table 2 shows that the first members of the Q_{Nlm} superseries with higher N values lie in the left half-plane of the complex R-plane. Also seen in this table is the irregularity of the values of Massey parameters $\Delta_0^{(Q)}$ within a given Q-superseries. This is a consequence of the fact that different members of these superseries connect molecular states which may asymptotically correlate with atomic states localized either on the same or on different Coulomb centres. We note that the values of $\Delta_0^{(Q)}$ are related to $\mathrm{Im}R_c^{(Q)}$ by (Grozdanov and Solov'ev 1990)

$$\Delta_0^{(Q)} \simeq \tfrac{1}{4}\pi |\Delta E_{\alpha\beta}(\mathrm{Re}R_c^{(Q)})\mathrm{Im}R_c^{(Q)}|. \tag{6}$$

We further note that the pairs of states 6hσ–7iσ, 8iσ–9jσ, 7gσ–8hσ, 5gπ–6hπ, 8jπ–9kπ and 7hπ–8iπ are coupled by both a Q-type and an isolated branching point (see table 2) of which only the latter are shown in figure 3.

3. Method of cross section calculations

In the advanced adiabatic approach to one-electron ion–atom collision systems one first introduces a non-stationary length transformation by the relation

$$\vec{r} = R(t)\vec{q} \tag{7}$$

where $\vec{r}$ is the electron coordinate with respect to the midpoint of the time depending internuclear distance $R(t)$, which transforms the adiabatic two-Coulomb centre Hamiltonian

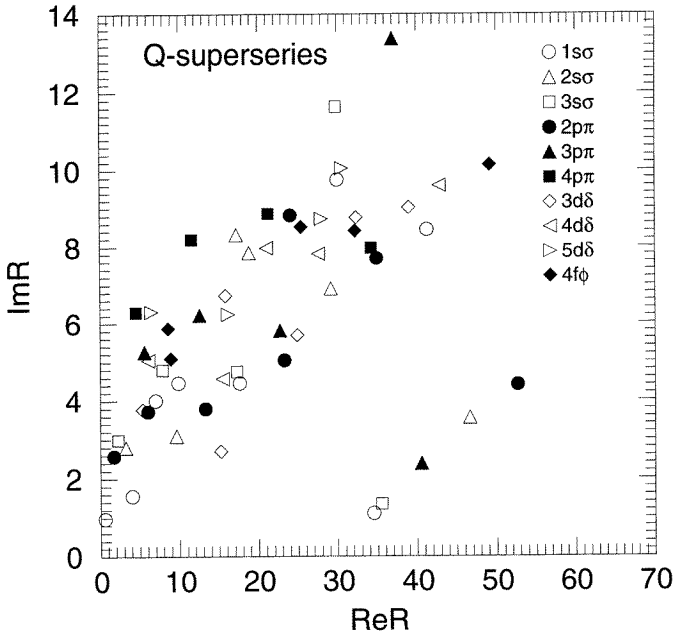

Figure 3. Positions of branching points $R_c^{(Q)}$ of several Q_{Nlm} superseries in the complex R-plane. The point with smallest $\mathrm{Re}R_c^{(Q)}$ within a given superseries (same symbol) represents the first point of that superseries in the $\mathrm{Re}R > 0$ half-plane. The points with $\mathrm{Re}R > 30$ and small imaginary part ($\mathrm{Im}R_c \ll \mathrm{Re}R_c$) represent isolated (Landau–Zener) branch points.

into an effective Hamiltonian

$$\tilde{H}(R) = -\tfrac{1}{2}\nabla_q^2 - \frac{Z_1 R}{|\vec{q} + \hat{\boldsymbol{R}}/2|} + \frac{Z_2 R}{|\vec{q} - \hat{\boldsymbol{R}}/2|} + \omega L_3 + \tfrac{1}{2}\omega^2 q^2 \tag{8}$$

where $\hat{\boldsymbol{R}}$ is a unit vector along the internuclear axis, L_3 is the operator of the projection of electron angular momentum onto the direction perpendicular to the collision plane and $\omega = bv$ (b, as before, being the impact parameter). After introducing an additional time transformation, $\tau = \arctan(vt/b)/\omega$, the original time-dependent Schrödinger equation (with moving Coulomb centres) is transformed into a modified Schrödinger equation with Coulomb centres staying at rest, i.e. the new dynamical adiabatic wavefunctions exhibit correct asymptotic behaviour.

The last two (dynamical) terms of the effective Hamiltonian (8) prevent the separation of variables in the corresponding eigenvalue problem. However, in the framework of the adiabatic approach we can consider the dynamical interactions in equation (8) as a perturbation. It can be easily shown (Solov'ev 1989) that the first-order corrections to the adiabatic energies caused by this perturbation are proportional to v^2 and, therefore, the Massey parameter Δ in the dynamical adiabatic basis has the form $\Delta = \Delta^{(0)} + v^2\Delta^{(1)} + \mathrm{O}(v^3)$, where $\Delta^{(0)}$ is the Massey parameter calculated within the standard two-Coulomb centre adiabatic basis. The corresponding transition probability is then given by the expansion $p_{\beta\alpha} = p_{\beta\alpha}^{(0)}(1+\mathrm{O}(v))$, i.e. in the region of validity of adiabatic approximation both basis sets give the same result for $p_{\alpha\beta}$. This is, however, not the case in the regions $R \to 0$ and $R \to \infty$, where strong Coulomb degeneracies occur. In these regions the dynamical perturbations in equation (8) change the adiabatic states already in the zeroth order. These

changes represent the effects of rotational couplings in the new, modified representation. In the $R \to 0$ limit the problem reduces to the mixing of states with different m within a given (N, l) manifold and can be solved by the close-coupling method (Grodzanov and Solov'ev 1982). In the region $R \to \infty$, the degeneracies can be removed completely only in the second-order perturbation theory in ω (Grozdanov and Solov'ev 1991). We note, however, that in this order of the perturbation theory the dynamical adiabatic wavefunctions are obtained exactly and their expansion over the spherical hydrogen-like states can be carried out analytically.

Knowing the elementary transition probabilities $p_{\alpha\beta}$ at each branching point R_c, equations (1)–(3), one can easily construct the adiabatic evolution matrix by a multiplicative procedure assuming that the interference effects between different reaction paths can be neglected (see e.g. Janev and Krstić 1992). The neglect of these effects can be justified in the total channel cross sections if the collision velocity is sufficiently small (Richter and Solov'ev 1993). The construction of the adiabatic evolution matrix includes also transformation of the separated atom spherical states into Stark states, the rotational transitions between the Stark states in both the entrance and exit channels and the rotational transitions in the united atom limit within each (N, l) manifold. In the present calculations, the rotational transitions at large internuclear distances have been calculated in the second-order perturbation theory with respect to the parameter ω, while the rotational transitions at small internuclear distances have been calculated by numerical solution of the corresponding close-coupled equations (Grozdanov and Solov'ev 1982). The evolution matrix also includes the ionization probabilities along the S- and Q-superseries. The cross sections of different reaction channels are calculated by integration of channel probabilities over the impact parameters. The determination of adiabatic energy branching points R_c, the calculation of the values of corresponding Massey parameters, the construction of the evolution matrix for a given basis set $\{N\}$ and the calculation of the channel and total cross sections for excitation, ionization and electron capture processes in the $Li^{3+} + H$ system with $N \leqslant 10$ has been performed by the computer program package ARSENY (see e.g. Solov'ev (1991) and Richter and Solov'ev (1993)). The results of cross section calculations are presented in the next two sections.

4. Cross section results for Li^{3+}+H(1s) collisions

4.1. Electron capture

In the adopted molecular basis for the $Li^{3+}+H$ system containing all the states with $N \leqslant 10$ ($l \leqslant N-1, m \leqslant l$) we have found 24 S-superseries with more than 70 branch points, and 30 Q-superseries with more than 100 branch points. Only a part of these superseries is shown in tables 1 and 2 and in figures 2 and 3. Besides, six isolated Landau–Zener pseudo-crossings were found in the considered system of molecular states (denoted by an asterix in table 2). When two adiabatic states are coupled by both a Q-type and an isolated branching point, the transition probability between the coupled states is calculated only with the (smaller) Massey parameter of the isolated branching point, since, in the spirit of the theory of asymptotic expansions, the inclusion of the contribution from the Q-branching point would mean in this case an overestimation of the accuracy of the method. The separated atom states which are included in the adopted molecular basis have principal quantum numbers $n \leqslant 3$ for the H^+ centre and $n \leqslant 9$ for the Li^{3+} centre. We should point out, however, that not all the molecular states (namely those with $N > 10$) which correlate with $n = 3$ states on H^+ and $n = 9$ states on Li^{3+} are present in our basis. Therefore, the excitation transitions to

H($n = 3$) and electron capture transitions to $Li^{2+}(n = 9)$ cannot be fully accounted for by the present calculations.

The initial molecular state of $Li^{3+} + H(1s)$ system is $3d\sigma$ and, as can be seen from table 2, it is strongly coupled with the $2p\sigma$ state, which asymptotically correlates with the $Li^{2+}(n = 2)$ manifold and with the $4f\sigma$ state, which asymptotically correlates with the $Li^{2+}(n = 3)$ manifold. Although the strength of the $3d\sigma$–$2p\sigma$ coupling is stronger than that of the $3d\sigma$–$4f\sigma$ coupling (see the corresponding Δ_0 values in table 2), the cross section for population of the $4f\sigma$ state at low energies is still larger than that for population of $2p\sigma$, since the $3d\sigma$–$4f\sigma$ coupling occurs at larger internuclear distances ($\mathrm{Re}R_c \simeq 7$). The population of $Li^{2+}(1s)$ electron capture channel is strongly inhibited by the large value of Massey parameter for the $2p\sigma$–$1s\sigma$ transition ($\Delta_0 = 2.7856$) and the small value of characteristic distance for this transition ($\mathrm{Re}R_c \simeq 0.6$). The population of $L^{2+}(n \geqslant 4)$ states requires a sequence of successive transitions along the $Q_{1s\sigma}$ superseries during the outgoing stage of the collision ($3d\sigma \rightarrow 4f\sigma \rightarrow 5g\sigma$ for $Li^{2+}(n = 4)$, $3d\sigma \rightarrow 4f\sigma \rightarrow 5g\sigma \rightarrow 6h\sigma$ for $Li^{2+}(n = 5)$, etc) and, therefore, the population probabilities for these states are correspondingly smaller than those for the $L^{2+}(n = 2, 3)$ states. Additional reaction paths for population of $Li^{2+}(n = 2, 3)$ manifolds are opened via the $2p\sigma$–$2p\pi$ (for $Li^{2+}(n = 2)$) and $3d\sigma \rightarrow 3d\pi \rightarrow 3d\delta$ (for $Li^{3+}(n = 3)$) rotational couplings at small internuclear distances. The $Q_{2p\pi}$, $Q_{3d\pi}$ and $Q_{3d\delta}$ superseries, initiated by these rotational transitions, provide a mechanism for population of the π- and δ-states of $Li^{2+}(n \geqslant 4)$ manifolds. The transitions at the lower S-branching points can also activate Q-superseries for population of higher n capture states. Thus, the $3d\sigma$–$4d\sigma$ S-transition at $\mathrm{Re}R_c \simeq 1.5$ activates the $Q_{4d\sigma}$-superseries (a sub-series of $Q_{2s\sigma}$), which populates the $n \geqslant 4$ manifolds of Li^{2+}. Obviously, the branching of probability flux in the transition region of any type (S- or Q-branching point, or rotational coupling at small R), creates a large number of reaction paths for population of a specific exit reaction channel. Generally speaking, however, only those reaction paths which include a small number of couplings give significant contribution to the cross section of a particular reaction channel. The contributing role of different couplings to the cross section may, of course, change when varying the collision velocity. Figure 4 shows the total electron capture cross section for $Li^{3+} + H(1s)$ collisions in the energy range 0.1–20 keV/u. The results of present calculations are in good agreement with those of the previous extensive AO- or MO-based close-coupling calculations mentioned in the introduction, but lie below the experimental data of Seim *et al* (1981) by 10–20% in the overlapping energy range. The reason for this disagreement could be either the neglected interference effects in the present treatment, or the neglect of rotational transitions in the united atom region for internuclear distances larger than the 'radii' of the S-superseries. In the region around 20 keV/u, the present results agree well with the cross section measurements of Shah *et al* (1978).

In figure 5 we present the calculated cross section for electron capture to specific n-shells of Li^{2+} ion. The partial cross sections for population of $n = 2$ and $n = 3$ shell are compared with the 24+ AO close-coupling results of Fritsch and Lin (1982). We note that the charge-exchange states with $Li^{2+}(n \geqslant 4)$ were not included in the AO-basis of Fritsch and Lin. The agreement of the two sets of calculations is quite good, except for the $n = 2$ case in the energy region below 1 keV/u. This fact is understandable in view of the small values of the cross sections for capture to $n \geqslant 4$ states. Both calculations show that in the region below approximately 1 keV/u, the dominant electron capture channel is $n = 3$. As mentioned at the beginning of this section, this is a consequence of the strong coupling between $3d\sigma$ and $4f\sigma$ molecular states in the region $\mathrm{Re}R \simeq 7$. In table 3 we give the calculated cross sections for electron capture to specific nl_a-subshells of the Li^{2+}

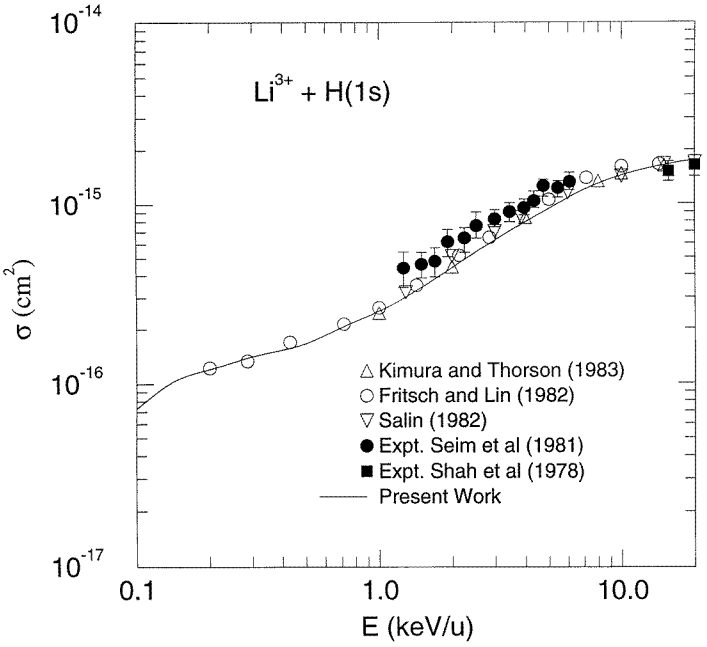

Figure 4. Total electron capture cross section in Li^{3+} + H(1s) collisions. The full curve represents the results of present calculations. The experimental data are indicated by closed symbols. The triangles and inverted triangles are the results of 10 MO and 24 MO close-coupling calculations, respectively, and the open circles are the results of 24 AO+ close-coupling calculations.

ion ($n = 2$–5) for a number of collision energies between 1 keV/u and 15 keV/u. (l_a designates the angular momentum quantum number of the atomic state). For $n = 2, 3$ and $E = 1, 5, 10$ keV/u the results of Fritsch and Lin (1982) are also shown in this table. There are significant differences between the two sets of cross section values, particularly for the energy of 1 keV/u. It is difficult to accurately trace the origin of these differences given the different character and size of the bases used in the two calculations. We note that the l_a-distribution of captured electrons within a given n-shell is dominantly determined by the rotational coupling of molecular states at large internuclear distances.

4.2. Excitation and ionization

The molecular states of Li^{3+}–H system, which in the separated atom limit go over to the H($n = 2$) manifold, are the 7iσ, 6gσ and 6hπ states. The 7iσ state can be populated by the $Q_{1s\sigma}$ superseries on the outgoing stage of the collision via the following sequence of transitions: 3d$\sigma \rightarrow$ 4f$\sigma \rightarrow$ 5g$\sigma \rightarrow$ 6h$\sigma \rightarrow$ 7iσ. As seen from table 2 the last step of this sequence of transitions is due to an isolated (Landau–Zener) branch point at $\mathrm{Re}R_x \simeq 34.5$ and it is, therefore, particularly strong ($\Delta_0 = 0.00145$). The 6gσ state can be populated by a 3d$\sigma \rightarrow$ 4dσ S-type transition during the incoming part of the trajectory, followed by the sequence of Q-type transitions 4d$\sigma \rightarrow$ 5f$\sigma \rightarrow$ 6gσ along the $Q_{2s\sigma}$ superseries during the outgoing stage of the collision. Finally, the 6hπ state is populated by the rotational 3dσ–3dπ transition in the united atom region, followed by the 3d$\pi \rightarrow$ 4f$\pi \rightarrow$ 5g$\pi \rightarrow$ 6hπ sequence of transitions along the $Q_{2p\pi}$ superseries. Again, the last transition in this sequence

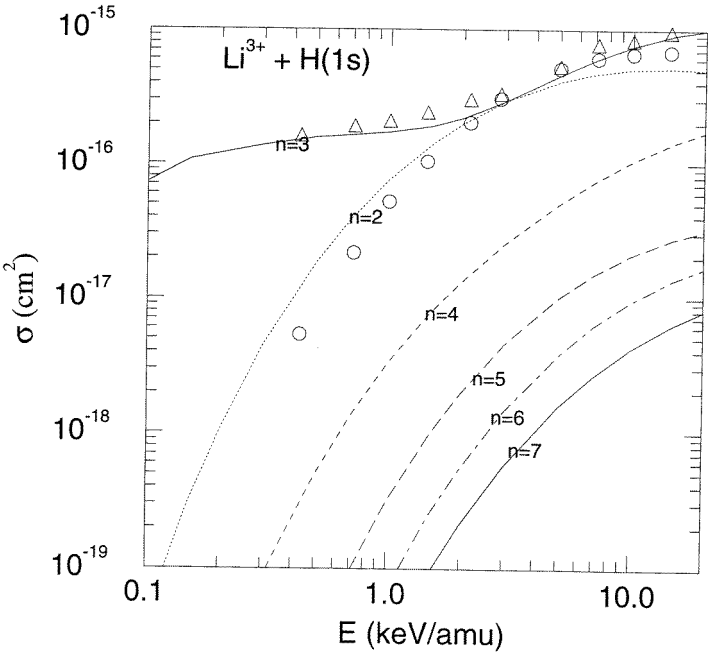

Figure 5. Cross section for electron capture into specific $Li^{2+}(n)$-shells in Li^{3+} + H(1s) collisions. The lines represent the results of present calculations. The symbols are the results of 24 AO+ close-coupling calculations of Fritsch and Lin (1982) for capture to $n = 2$ and $n = 3$ shells.

is an isolated branching point and is, therefore, very strong ($\Delta_0 = 0.093$; see table 2). The fact that all intermediate states in the above transition sequences are connected with the $Li^{2+}(n = 3, 4, 5)$ electron capture channels makes the excitation of the H($n = 2$) manifold a weak process. On the other hand, the strong 6h$\sigma \rightarrow$ 7iσ and 5g$\pi \rightarrow$ 6hπ transitions prevent a considerable population of the $Li^{2+}(n = 5)$ charge exchange states.

As has been mentioned in section 3, our $N \leqslant 10$ molecular basis includes the 9iσ, 9jπ, 9kδ, 10kσ and 10lπ states which asymptotically correlate with the H($n = 3$) manifold, but does not include the state 11mσ which also correlates to the same manifold. The $n = 3$ excitation state 11mσ can be reached by continuing the evolution along the $Q_{1s\sigma}$ superseries from the 7iσ $n = 2$ excitation state. Since in the excitation of 11mσ, 10lπ and 10kσ states four successive transitions are needed (e.g. 7i$\sigma \rightarrow$ 8j$\sigma \rightarrow$ 9k$\sigma \rightarrow$ 10l$\sigma \rightarrow$ 11mσ, in the case of the $Q_{1s\sigma}$ superseries), it can be expected that the population of these excited states would be considerably smaller than that of 7iσ, 6hπ and 6gσ $n = 2$ excited states. The population of the other three molecular states, 9iσ, 9jπ and 9kδ, which in the separated atom limit correlate with the H($n = 3$) manifold, also includes sequences of a large number of transitions. For instance, the 9iσ state can be populated by making the 3d$\sigma \rightarrow$ 4d$\sigma \rightarrow$ 5dσ S-type transitions during the incoming part of the trajectory and the 5d$\sigma \rightarrow$ 6f$\sigma \rightarrow$ 7g$\sigma \rightarrow$ 8h$\sigma \rightarrow$ 9iσ Q-type transitions during the outgoing part of the trajectory. Therefore, these $n = 3$ excitation channels are also expected to be weak.

In table 4 we give the calculated cross sections for excitation of 2s and 2p states of hydrogen atom in the energy range 1–20 keV/u. For a number of collision energies the present cross sections are compared with those of 24 AO close-coupling calculations of

Table 3. Cross sections (in units of 10^{-16} cm^2) for the $Li^{3+}+H(1s) \rightarrow Li^{2+}(nl_a)+H^+$ reaction ($n = 2$–5). (The values in square brackets are the results of Fritsch and Lin (1982).)

		E				
n	nl_a	1 keV/u	2 keV/u	5 keV/u	10 keV/u	15 keV/u
2	2s	1.91(−1)[a]	5.03(−1)	1.04	1.29	1.32
		[2.46(−1)]		[2.32]	[2.01]	
	2p	5.68(−1)	1.49	3.08	3.82	3.88
		[2.76(−1)]		[2.81]	[4.59]	
3	3s	4.00(−1)	4.16(−1)	5.45(−1)	7.40(−1)	8.50(−1)
		[2.08(−1)]		[8.13(−1)]	2.69	
	3p	2.99(−1)	5.09(−1)	1.49	4.14	3.33
		[8.37(−1)]		[1.94]		
	3d	1.03	1.28	2.54		5.01
		[1.05]		[2.61]		
4	4s	3.42(−3)	1.36(−2)	4.37(−2)	7.56(−2)	9.40(−2)
	4p	6.61(−3)	2.39(−2)	7.92(−2)	1.64(−1)	2.31(−1)
	4d	8.89(−3)	3.54(−2)	1.52(−1)	3.60(−1)	5.24(−1)
	4f	1.42(−2)	5.69(−2)	2.26(−1)	4.56(−1)	6.08(−1)
5	5s	2.71(−4)	1.57(−3)	7.19(−3)	1.45(−2)	1.90(−2)
	5p	6.37(−4)	3.71(−3)	1.53(−2)	2.72(−2)	3.30(−2)
	5d	7.52(−4)	4.33(−3)	1.95(−2)	4.00(−2)	5.39(−2)
	5f	8.48(−4)	5.48(−3)	2.83(−2)	6.02(−2)	8.00(−2)
	5g	6.27(−4)	4.78(−3)	2.99(−2)	6.81(−2)	9.14(−2)

[a] $a(-x) = a \times 10^{-x}$.

Table 4. Excitation and ionization cross sections (in units of 10^{-16} cm^2) for $Li^{3+} + H(1s)$ collisions. (The values in square brackets are the results of Bransden and Noble (1982).)

E (keV/amu)	$\sigma_{ex}(2s)$	$\sigma_{ex}(2p)$	σ_{ion}
1.0	1.51(−3)[a]	2.26(−3)	3.70(−4)
1.5	4.93(−3)	6.90(−3)	1.90(−3)
	[2.0(−2)]	[5.5(−2)]	
2.0	1.01(−2)	1.42(−2)	5.14(−3)
3.0	2.47(−2)	3.74(−2)	1.75(−2)
5.0	6.74(−2)	1.25(−1)	6.31(−2)
	[1.8(−1)]	[2.2(−1)]	
7.0	1.24(−1)	2.64(−1)	1.29(−1)
10.0	2.27(−1)	5.43(−1)	2.48(−1)
	[1.6(−1)]	[3.0(−1)]	
15.0	4.17(−1)	1.09	4.65(−1)
20.0	6.06(−1)	1.65	6.81(−1)

[a] $a(-x) = a \times 10^{-x}$.

Bransden and Noble (1982). The differences between the two sets of data, particularly for $E = 1.5$ keV/u and $E = 5$ keV/u, are considerable. The application of the AO close-coupling model at these low energies is, however, not expected to be justifiable. It should be noted that in the region above approximately 7 keV/u, the 2s and 2p excitation cross sections calculated by the present method are larger than those of Bransden and Noble

(1982). (For $E \leqslant 7$ keV/u the opposite is true.) This is a consequence of the fact that the atomic basis used in the calculations of Bransden and Noble includes all the $n = 3$ states (and, therefore, a larger part of the excitation flux is transmitted from $n = 2$ to $n = 3$ states), which is not the case with the basis used in the present calculations.

In table 4 we also give the results for ionization of H(1s) by Li^{3+} ions in the same energy range. The main contribution to the ionization cross section at energies below approximately 5 keV/u give the $S_{p\sigma}$, $S_{d\sigma}$ and $S_{f\sigma}$ superseries, while for higher energies the ionization via the $Q_{1s\sigma}$, $Q_{2s\sigma}$ and $Q_{2p\pi}$ superseries also becomes important. In the upper part of this energy range, the ionization cross section becomes less reliable since it may include a significant fraction of the excitation and charge exchange channels to states with $N \geqslant 11$, treated here as lying in the continuum.

5. Li^{3+}+H(2s) collisions

5.1. Charge exchange

The initially occupied 7iσ and 6gσ molecular states of $Li^{3+} + H(2s)$ system are rotationally coupled with the 6hπ state at large distances and, thus, the system enters the molecular collision region with three initial molecular states, 7iσ, 6gσ and 6hπ (with well defined populations). These three states exhibit very strong couplings 7iσ–6hσ, 6gσ–5fσ, 6hπ–5gπ with the $Li^{2+}(n = 5)$ charge exchange states already at large internuclear distances (at $Re R_c \simeq 34.5$, $Re R_c \simeq 17.2$ and $Re R_c \simeq 23.3$, respectively). The Massey parameter values of these couplings are 0.0014, 0.13 and 0.093, respectively (see table 2). In their turn, the 6hσ, 5fσ and 5gπ molecular states also have strong couplings with the $Li^{2+}(n = 4)$ 5gσ, 4dσ and 4fπ charge exchange states, respectively, still at sufficiently large distances (see table 2). Therefore, most of the initial-state population is transferred to the $Li^{2+}(n = 4)$ 5gσ, 4dσ and 4fπ charge exchange states already in the incoming part of the collision. These circumstances lead to dominant population of the $L^{2+}(n = 4, 5) + H^+$ charge exchange channels in slow $Li^{3+} + H(2s)$ collisions.

The total and n-selective electron capture cross sections for $Li^{3+} + H(2s)$ collisions, in the energy range 1–7 keV/u, are shown in figure 6. As argued above, the $n = 4, 5$ shells are populated dominantly, with $n = 4$ being the dominant channel for $E > 0.5$ keV/u and $n = 5$ dominating for $E < 0.5$ keV/u. The open symbols in this figure are the results of Landau–Zener model calculations of Casaubon and Piacentini (1984) with the 6hσ–5gσ and 5fσ–4dσ radial couplings only (i.e. assuming that the 7iσ–6hσ and 6gσ–5fσ transitions in the incoming part of the trajectory have a unit probability). Since the 5gσ and 4dσ molecular states in the separated atom limit go over into the $Li^{2+}(n = 4)$ manifold of states, the cross sections of Casaubon and Piacentini are pertinent to the $n = 4$ channel only. With this in mind, their agreement with our results for the $n = 4$ channel can be considered quite satisfactory.

The cross sections for capture into specific $Li^{2+}(nl_a)$ states for $n = 4, 5, 6, 7$, are given in table 5 for a number of collision energies between 0.2 and 3 keV/u. As in the Li^{3+}+H(1s) case, the l_a-distributions of captured electrons within a given n-shell are determined by the rotational mixing of corresponding Stark states at large internuclear distances.

5.2. Excitation and ionization

As mentioned in section 4.2, the absence of the 11mσ state in our molecular basis prevents us calculating the excitation to the $H(n = 3)$ states exactly. However, the flux reaching this

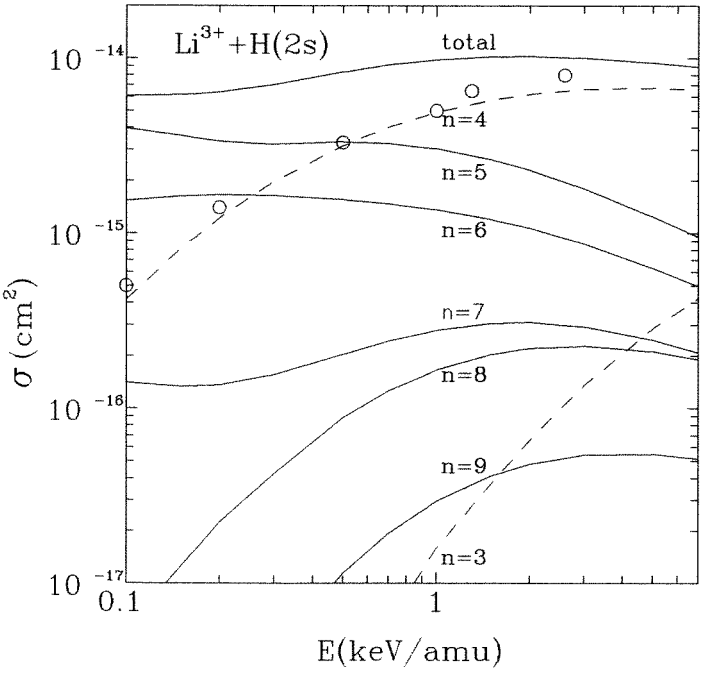

Figure 6. Total and shell-selective electron capture cross sections in $Li^{3+}+H(2s)$ collisions. The lines represent the results of present calculations. The open circles are the results of two-channel Landau–Zener model calculations of Casaubon and Piacentini (1984).

state is expected to be small with respect to the total flux reaching the $n = 3$ manifold (e.g. four intermediate transition steps along the $Q_{1s\sigma}$ series are required to reach $11m\sigma$ from $7i\sigma$). In table 6 we give the cross section for excitation of the $n = 3$ manifold (disregarding the contribution from the state $11m\sigma$) in the energy range 0.1–7 keV/u. We note that for $E \leqslant 2$ keV/u more than 90% of the cross section comes from the population of the 3d atomic state, and that for $E = 7$ keV/u the 3d contribution to $n = 3$ excitation amounts to 86%. The $n = 3$ excitation cross section shows a maximum around $E \simeq 0.7$ keV/u. The cross section for the $2s \rightarrow 2p$ transition is also given in table 6. In the considered energy range, the $2s \rightarrow 2p$ excitation cross section weakly depends on the energy and shows a broad maximum around 5 keV/u. The high cross section values for the $2s \rightarrow 2p$ excitation are, of course, not surprising, because of the strong mixing of 2p-state Stark components with those of the initial state at large internuclear distances. It should, however, be noted that this mixing is not sufficiently strong to produce a statistical l_a-distribution within the final $n = 2$ manifold: the 2p excitation cross section is only about a factor of two larger than the cross section of the elastic channel.

The cross section for ionization in $Li^{3+}+H(2s)$ slow collisions is also given in the same table. In the upper part of the considered energy range ($E \geqslant 2$ keV/u), the ionization cross section should be considered as less accurate because it includes a contribution from the excitation and electron capture transitions to asymptotic states which correlate with $N \geqslant 11$ molecular states.

Table 5. Cross sections for capture into nl_a-states in $Li^{3+} + H(2s)$ collisions (in units of 10^{-16} cm^2).

		E					
n	nl_a	0.2 keV/*u*	0.5 keV/*u*	0.7 keV/*u*	1 keV/*u*	2 keV/*u*	3 keV/*u*
4	4s	1.36	3.37	4.39	5.33	5.66	4.83
	4p	3.22	8.81	1.12(+1)[a]	1.38(+1)	1.76(+1)	1.82(+1)
	4d	3.45	7.92	9.22	1.05(+1)	1.49(+1)	2.00(+1)
	4f	4.13	1.16(+1)	1.54(+1)	1.95(+1)	2.40(+1)	2.33(+1)
5	5s	1.16	1.86	2.45	2.84	2.34	1.67
	5p	5.65	5.46	5.34	5.12	4.32	3.48
	5d	9.19	8.86	8.10	6.60	3.68	2.74
	5f	9.21	6.79	6.68	6.85	6.47	5.43
	5g	8.31	1.04(+1)	1.01(+1)	9.05	6.20	4.72
6	6s	2.22(−1)	2.50(−1)	2.93(−1)	3.63(−1)	4.30(−1)	3.84(−1)
	6p	3.13(−1)	4.73(−1)	5.51(−1)	6.35(−1)	7.25(−1)	6.64(−1)
	6d	7.97(−1)	1.10	1.19	1.22	1.11	1.05
	6f	2.55	2.32	2.21	2.09	1.69	1.35
	6g	5.22	4.48	3.99	3.42	2.50	2.11
	6h	7.49	6.95	6.52	5.89	4.22	3.14
7	7s	1.40(−2)	3.34(−2)	4.66(−2)	6.51(−2)	8.87(−2)	8.40(−2)
	7p	2.11(−2)	5.68(−2)	7.16(−2)	8.29(−2)	1.01(−1)	1.11(−1)
	7d	5.16(−2)	1.27(−1)	1.68(−1)	2.11(−1)	2.58(−1)	2.57(−1)
	7f	1.20(−1)	2.10(−1)	2.53(−1)	2.95(−1)	3.47(−1)	3.38(−1)
	7g	2.32(−1)	3.62(−1)	4.36(−1)	5.02(−1)	5.24(−1)	4.79(−1)
	7h	3.87(−1)	5.10(−1)	5.89(−1)	6.67(−1)	7.34(−1)	6.98(−1)
	7i	5.35(−1)	7.39(−1)	8.64(−1)	9.83(−1)	1.05	9.70(−1)

[a] $a(\pm x) = a \times 10^{\pm x}$.

6. Concluding remarks

In the present paper we have studied the low-energy inelastic processes in $Li^{3+} + H(1s)$ and $Li^{3+} + H(2s)$ systems by using the advanced adiabatic method. The molecular basis used in the calculations ($N \leqslant 10$) was sufficient to describe all electron capture channels up to $n = 9$ on Li^{2+}, but insufficient to include the target excitation to $n = 3$ state and above. The ionization channels were defined by transitions to states with $N \geqslant 11$.

In the case of $Li^{3+} + H(1s)$ collisions, the calculated total electron capture cross section was found to agree well with the results of previous AO- and MO-large-base close-coupling calculations. The present results for the shell and subshell selective electron capture and excitation cross sections are also in general agreement with the AO-based close-coupling calculations, except in the region of below approximately 5 keV/*u* where the AO-models are expected to be less adequate for description of collisional dynamics.

The total electron capture cross section for $Li^{3+} + H(2s)$ collisions in the energy range 0.1–7 keV/*u* was found to be significantly larger than the previous results of Casaubon and Piacentini (1984), based on a two-channel Landau–Zener model. However, since the two considered molecular charge exchange channels both contribute to the population of the $Li^{2+}(n = 4)$ only, the electron capture cross section of Casaubon and Piacentini is consistent with the present results for the same channel. The excitation and ionization cross

Table 6. Excitation and ionization cross sections (in units of 10^{-16} cm^2) in Li^{3+} + H(2s) collisions.

E (keV/u)	$\sigma_{ex}(2s \rightarrow 2p)$	$\sigma_{ex}(2s \rightarrow n = 3)$	σ_{ion}
0.1	3.65(+1)[a]	4.72(−1)	2.67(−2)
0.15	3.79(+1)	5.71(−1)	6.24(−2)
0.2	3.97(+1)	7.27(−1)	1.21(−2)
0.3	4.45(+1)	9.30(−1)	3.17(−1)
0.5	5.43(+1)	1.07	9.43(−1)
0.7	6.14(+1)	1.08	1.82
1.0	6.88(+1)	1.03	3.34
1.5	7.62(+1)	9.00(−1)	5.94
2.0	8.04(+1)	7.86(−1)	8.29
3.0	8.43(+1)	6.28(−1)	1.20(+1)
5.0	8.42(+1)	4.62(−1)	1.65(+1)
7.0	8.16(+1)	3.77(−1)	1.87(+1)

[a] $a(\pm x) = a \times 10^{\pm x}$.

sections for Li^{3+}–H(1s), H(2s) collisions at the considered low energies, are considerably smaller compared with the electron capture cross sections, as should be expected.

The upper limit of the energy range of present calculations was determined on the basis of Massey adiabatic criterion $v \lesssim \Delta_{eff}$, where Δ_{eff} is a certain effective Massey parameter for a considered reaction channel. In practice, this criterion limits the validity of cross section results for a particular channel to collision energies where the cross section takes its maximum. The lower limit of the energy range for our calculations was determined by the estimated limit of validity of the adopted straightline trajectory approximation for the nuclear motion.

The adiabatic method used in the present calculations is expected to provide increasingly more accurate results with decreasing collision velocity. The main source of uncertainty at larger collision velocities is the neglect of the v-dependence of the Massey parameter, $\Delta = \Delta_0 + O(v^2)$, and the quantum interference effects, the magnitude of which in the total cross sections is also of the order of $O(v^2)$. Within these limitations, the advanced adiabatic method based on the dynamical adiabatic molecular states and analytical properties of adiabatic energy surfaces in the complex R-plane provides a transparent picture of the collision dynamics in one-electron ion–atom(ion) collision systems. It should be mentioned that the advanced adiabatic approach conceptually is not limited to one-electron two-Coulomb centre problems. Both of its essential ingredients, namely the introduction of the dynamical adiabatic basis and the analytical continuation of the potential energies in the complex R-plane, are independent of the number of electrons in the collision system and are only related to the Born–Oppenheimer separation of nuclear and electronic motions. The method can also be generalized to multi-centre collision systems. The first generalizations of the method along these lines have just begun (Krstić 1995).

Acknowledgment

One of us (EAS) would like to acknowledge the support of the International Atomic Energy Agency received under the research contract 8610/RB.

References

Aumayr F, Schorn R P, Pöckle M, Schweinzer J, Wolfrum E, McCormick K, Hintz E and Winter H P 1992 *J. Nucl. Mater.* **196–198** 928

Bransden B H and Noble C J 1982 *J. Phys. B: At. Mol. Phys.* **15** 451–5

Casaubon J I and Piacentini R D 1984 *J. Phys. B: At. Mol. Phys.* **17** 1623–30

Fisher R K, McChesney J M, Parks P B, Duong H H, Medley S S, Roquemore A L, Mansfield D K, Budney R V, Petrov M P and Olson R E 1995 *Phys. Rev. Lett.* **75** 846–9

Fritsch W and Lin C D 1982 *J. Phys.* B **15** L281–7

Grozdanov T P and Solov'ev E A 1982 *J. Phys. B: At. Mol. Phys.* **15** 3871

——1990 *Phys. Rev.* A **42** 2703

——1991 *Phys. Rev.* A **44** 5604

Janev R K and Krstić P S 1991 *Phys. Rev.* A **44** R1436

——1992 *Phys. Rev.* A **46** 5554

Kimura M and Thorson W R 1983 *J. Phys. B: At. Mol. Phys.* **16** 1471–80

Krstić P S 1995 *19th Int. Conf. Phys. Electron. Atomic Collisions: Scientific Program and Abstracts of Contributed Papers* ed J B A Mitchell, J W McConkey and C E Brion (Canada: Whistler) vol 2, p 621

Krstić P S and Janev R K 1993 *Phys. Rev.* A **47** 3894–912

Krstić P S, Radmilović M and Janev R K 1992 *At. Plasma-Mat. Int. Data Fusion (Nucl. Fusion Suppl.)* **3** 113–25

Lüdde H J and Dreizler R M 1982 *J. Phys.* B **15** 2713–20

Ovchinnikov S Yu and Solov'ev E A 1986 *Zh. Eksp. Teor. Fiz.* **90** 921; (Eng. transl. 1986 *Sov. Phys.–JETP* **64** 280)

Richter K and Solov'ev E A 1993 *Phys. Rev.* A **48** 432

Salin A 1982 *Phys. Lett.* **91A** 61–3

Seim W, Müller A, Wirkner-Bott I and Salzborn E 1981 *J. Phys. B: At. Mol. Phys.* **14** 3475–91

Shah M B, Goffe T V and Gilbody H B 1978 *J. Phys. B: At. Mol. Phys.* **11** L233–6

Solov'ev E A 1981 *Zh. Eksp. Teor. Fiz.* **81** 1681 (Engl. transl. 1981 *Sov. Phys.–JETP* **54** 893)

——1986 *Zh. Eksp. Teor. Fiz.* **90** 1165 (Engl. transl. 1986 *Sov. Phys.–JETP* **63** 678)

——1989 *Usp. Fiz. Nauk.* **157** 437 (Engl. transl. 1989 *Sov. Phys.–Usp.* **32** 228)

——1991 *Workshop on Hidden Crossings in Ion–Atom Collisions and in other Nonadiabatic Transitions* Harvard-Smithsonian Center for Astrophysics, Cambridge p 27